Copyright by the American Institute of Physics (AIP). Wang, Z.; Wang, Y.; Ge, W.; et al., “Volatile and nonvolatile magnetic easy-axis rotation in epitaxial ferromagnetic thin films on ferroelectric single crystal substrates,” Appl. Phys. Lett. 103, 132909 (2013); http://dx.doi.org/10.1063/1.4823539

Volatile and nonvolatile magnetic easy-axis rotation in epitaxial ferromagnetic thin films on ferroelectric single crystal substrates

Z. Wang, Y. Wang, W. Ge, J. Li, and D. Viehland

Citation: Applied Physics Letters **103**, 132909 (2013); doi: 10.1063/1.4823539
View online: http://dx.doi.org/10.1063/1.4823539
View Table of Contents: http://scitation.aip.org/content/aip/journal/apl/103/13?ver=pdfcov
Published by the AIP Publishing

Re-register for Table of Content Alerts

Create a profile.

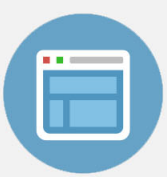

Sign up today!

This article is copyrighted as indicated in the article. Reuse of AIP content is subject to the terms at: http://scitation.aip.org/termsconditions. Downloaded to IP: 128.173.125.76 On: Mon, 13 Jan 2014 20:11:51

Volatile and nonvolatile magnetic easy-axis rotation in epitaxial ferromagnetic thin films on ferroelectric single crystal substrates

Z. Wang,[a] Y. Wang, W. Ge, J. Li, and D. Viehland
Department of Materials Science and Engineering, Virginia Tech, Blacksburg, Virginia 24061, USA

(Received 19 August 2013; accepted 10 September 2013; published online 25 September 2013)

We explored the relationship between phase transformation and magnetoelectric effect by depositing epitaxial $CoFe_2O_4$ films on ⟨110⟩ oriented $Pb(Mg,Nb)O_3$-$PbTiO_3$ (PMN-PT) with three different $PbTiO_3$ contents (PMN-28PT, PMN-29.5PT, and PMN-30PT). Electric-field controlled rhombohedral to orthorhombic phase transformation was confirmed by both piezoelectric and dielectric constant measurements. A giant in-plane (IP) uniaxial strain in $CoFe_2O_4$ film was induced due to dramatic lattice parameter change trigged by phase transition. Magnetic easy axis can be rotated from IP⟨110⟩ to IP⟨001⟩. More importantly, the phase transformation could be either reversible or irreversible, resulting in either volatile or nonvolatile magnetic easy axis rotations.
© *2013 AIP Publishing LLC*. [http://dx.doi.org/10.1063/1.4823539]

Tuning of magnetic anisotropy in ferromagnetic (FM) thin films by an electric-field induced strain in ferroelectric (FE) substrates is a converse magnetoelectric (ME) effect. This effect could be of significant importance due to potential applications in electric-write magnetic memories and electric-field-tunable microwave devices.[1–3] Strong coupling between ferroelectric and ferromagnetic phases can be achieved across their inter-phase interfaces through elastic strain mediation in composite ME structures, if a ferroelectric phase with a high electromechanical coupling coefficient and a ferromagnetic phase with a high magnetomechanical coupling coefficient are brought together in composite form.[4–7] A phenomenological approach has previously been used to calculate strain-induced magnetic easy-axis reorientation in various ferromagnetic thin films under electric-fields applied along different directions.[8–10] These studies have predicted the possible existence of a strain-mediated ME random access memory with ultra-high storage capacity, which has stimulated extensive investigations on the growth of epitaxial ferromagnetic thin films on ferroelectric substrates.[11–16]

However, electric-field induced strain in ferroelectric materials is a complex phenomena, where electric polarization rotation and reorientation coexist, and where linear piezoelectric strains are tenable only for modest electric-field ranges.[17,18] Non-180° domain reorientation and polarization rotation (i.e., monoclinic phase transitions) under electric field can trigger a step change of the crystal lattice parameters, and thus a large strain. Moreover, in consideration that strain is a tensor property, the question of how effective strain transfers between substrate and film must be kept in mind: this is because across the two dimensional interface between film and substrate, in-plane strain can be transferred, but not the out-of-plane component. Previously, ⟨110⟩ oriented $(1-x)Pb(Mg,Nb)O_3$-$xPbTiO_3$ (PMN-PT) crystals with large transverse piezoelectric (d_{31}) coefficients with FM thin films deposited on top have been shown to have significantly larger converse ME effects than ⟨001⟩ oriented ones with a larger longitudinal piezoelectric (d_{33}) coefficient when an electric-field is applied across the FM/FE heterostructure.[19,20] A few previous studies about ME effects in FM/FE heterostructures have considered PMN-PT substrates, but only as a linear piezoelectric strain source. However, another important property of ⟨110⟩ oriented PMN-PT crystals is the coexistence of both volatile and nonvolatile strains induced by electrically controlled phase transformations.

Here, we report the epitaxial growth of Mn-doped $CoFe_2O_4$ (MCFO) thin films on ⟨110⟩ oriented PMN-PT single crystals with different $PbTiO_3$ contents, and thus the particular case of substrates with different phase transition sequences. A systematic study of the reversible and irreversible electric-field induced strain effects on the tunable magnetic response of ferromagnetic thin films was then performed.

Epitaxial MCFO thin films with a thickness of ~200 nm were deposited on ⟨110⟩ oriented PMN-PT substrates with a dimension of $5 \times 5 \times 0.5$ mm^3 by pulsed laser deposition. Piezoelectric coefficients were measured using a Sinocera d_{33} METER (S5865). The M-H loops were measured using a Lakeshore vibrating sample magnetometer (7300) at room temperature.

Mn (20 at. %) doped CFO with a large saturation magnetization and high permeability was selected as the ferromagnetic phase due to its larger magnetic permeability.[7,21,22] PMN-PT single crystals were selected as the ferroelectric substrate due to ultrahigh electromechanical properties in the vicinity of the morphotropic phase boundary (MPB) owning to polarization rotation within a flat free energy profile.[23,24] Moreover, PMN-PT has a moderate lattice mismatch with ferromagnetic ferrites.[12]

In the $(1-x)$PMN-xPT solid solution, a spectrum of structures with different spontaneous polarization (P_s) directions can be "tuned" by $PbTiO_3$ content.[25] In addition, induced phase transformations and polarization direction rotations are well known to be induced by external electric fields, resulting in significant changes in the unit cell parameters.[18] Furthermore, the electrically induced strain due to polarization rotation can be volatile or nonvolatile as the intermediate M and orthorhombic (O) phases have different stabilities on removal of E for crystals with different compositions.[17] In the volatile case, the polar domains rotate back to their initial direction and recover their original state after removal of E;

[a]E-mail: zgwang@vt.edu

 © 2013 AIP Publishing LLC

This article is copyrighted as indicated in the article. Reuse of AIP content is subject to the terms at: http://scitation.aip.org/termsconditions. Downloaded to IP: 128.173.125.76 On: Mon, 13 Jan 2014 20:11:51

whereas in the nonvolatile one, the induced strain state is metastable and an energy barrier impedes the recovery of the original polarization direction on removal of E.

Figure 1 shows the evolution of the polarization direction with a field applied along ⟨110⟩ in the R phase PMN-PT substrate along out-of-plane (OP). Initially, there are eight possible polarization directions along the four body diagonals in the pseudo-cubic crystal cell. Next, an electric-field (E_{up}) along OP⟨110⟩ can degenerate these eight possible polarization directions into two acclivous ones with an inclined angle of ~35° from the poling field (Fig. 1(b)). As E_{up} is increased, the two possible acclivous polarization orientations tilt further towards the direction of E_{up}, resulting in a mono-domain O phase, as shown in Fig. 1(c). Upon removal of E_{up} two situations may occur: (i) a metastable mono-domain O phase might remain with polarization along ⟨110⟩; (ii) the polarization can rotate back to the ⟨111⟩ directions and recover the original R phase condition, as shown in Figs. 1(d) and 1(e). In the present investigation, PMN-PT substrates with three different PT contents of 28 at. %, 29.5 at. %, and 30 at. % (denoted as PMN-28PT, PMN-29.5PT, and PMN-30PT) were selected, which possessed varying degrees of volatile and nonvolatile strains.

Figure 1(f) shows the phase diagram of PMN-xPT under different electric fields of $-2 \le E \le 10$ kV/cm. PMN-28PT remained within the R-phase stability range, possessing a linear strain-E relationship.[26] PMN-29.5PT exhibited a R→O transform at E1 as the electric-field was increased, but recovered the original R-phase at E_2 as the electric-field was subsequently decreased ($0 \le E_2 \le E_1$).[27] PMN-30PT transformed from R→O phases at E_3 as the field was increased, and then recovered the original R phase at E_4 as a field of opposite sign was applied. ($E_4 \le 0 \le E_3$).[28] The relationship between the four threshold electric-fields (E_1 to E_4) was determined by dielectric constant measurement as a function of temperature in both heating and cooling process for the poled samples, where the dielectric constant flex points indicating ferroelectric phase transformations (see Figure S1).[29] To further confirm the phase stability of the PMN-PT crystals under different electric-fields, we measured the piezoelectric coefficient of each sample after poling under different electric-fields, as shown in Fig. 1(g). PMN-28PT and PMN-29.5PT exhibited a monotonically increasing value of d_{33} with step jumps near 1.2 and 1.5 kV/cm, respectively. However, the piezoelectric coefficient of PMN-30PT first experienced a rapid increasing range for $1.1 \le E \le 1.8$ kV/cm ($d_{33} = 1550$ pC/N @1.8 kV/cm), and then a rapid decreasing one for $2 \le E \le 2.5$ kV/cm. A low value of $d_{33} \approx 200$ pC/N was found for $E = 2.5$ kV/cm. The low value of d_{33} as the poling field was increased can be only attributed to the formation and stabilization of a mono-domain O phase.[30]

Figure 2 shows the magnetization hysteresis loops (M-H) for an epitaxial MCFO thin film grown on PMN-28PT. As the electric field increased, the polarization orientation was tilted towards OP, resulting in a compressive strain along IP⟨001⟩ and a tensile one along IP⟨110⟩. Figs. 2(a)–2(c) show variations in the M-H loops for data taken along IP⟨001⟩, IP⟨110⟩, and OP⟨110⟩, respectively. The MCFO layer has a negative magnetostriction along both ⟨100⟩ and ⟨110⟩,[9] thus a switching of the magnetic domains along IP⟨001⟩ will become increasingly difficult with increasing E due to a compressive strain. This will result in an increased remnant magnetization (M_r). On the contrary, along the IP⟨110⟩ and OP⟨110⟩, magnetic domain switching should become "softer" due to a tensile strain, resulting in a decreased M_r. Fig. 2(d) shows the M_r/M_s ratio (R_M) as a function of E applied along three directions. Initially, IP⟨110⟩ was the easy axis with $R_M \approx 3.9$, whereas the IP⟨001⟩ was the harder axis with $R_M \approx 2.6$. However, as the E applied out-of-plane was increased, a large anisotropic strain was induced in the MCFO film by the PMN-PT substrate. This resulted in a change in the magnetic response:

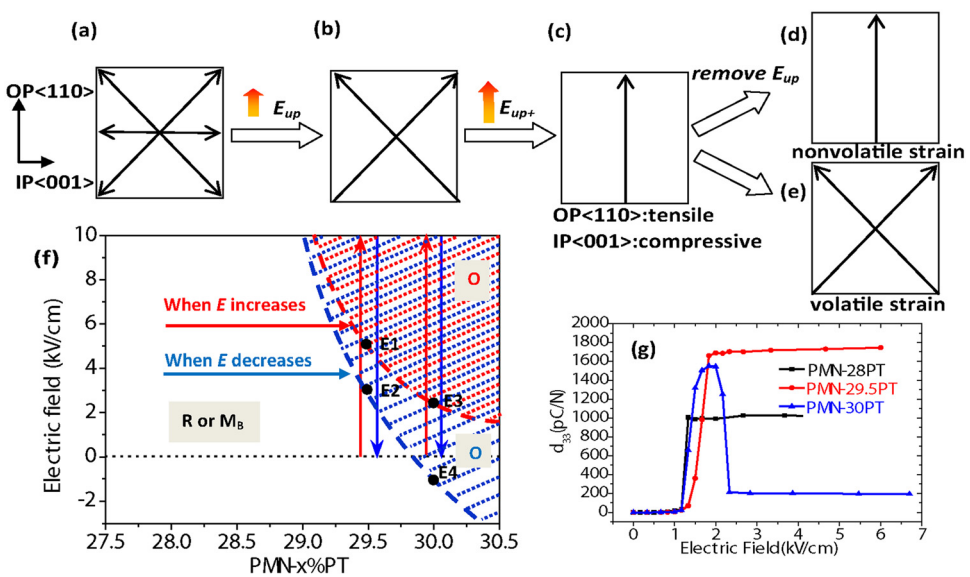

FIG. 1. Schematic illustrations of polarization rotation of ⟨110⟩ oriented PMN-PT under different electric-field. (a) Projection of intrinsic eight possible *P* directions seen from IP⟨110⟩ direction. (b) Two possible *P* directions degenerated by an upward electric field (E_{up}). (c) Further tilting of *P* directions towards the electric-field direction under an increasing electric field (E_{up+}) and formation of a mono-domain O-phase. (d) and (e) Two possible remaining ferroelectric domain configurations after removal of external electric-field. (f) Phase diagram of PMN-xPT at different electric-field. (g) Piezoelectric coefficient of PMN-PT crystals after different electric-field poling.

This article is copyrighted as indicated in the article. Reuse of AIP content is subject to the terms at: http://scitation.aip.org/termsconditions. Downloaded to IP: 128.173.125.76 On: Mon, 13 Jan 2014 20:11:51

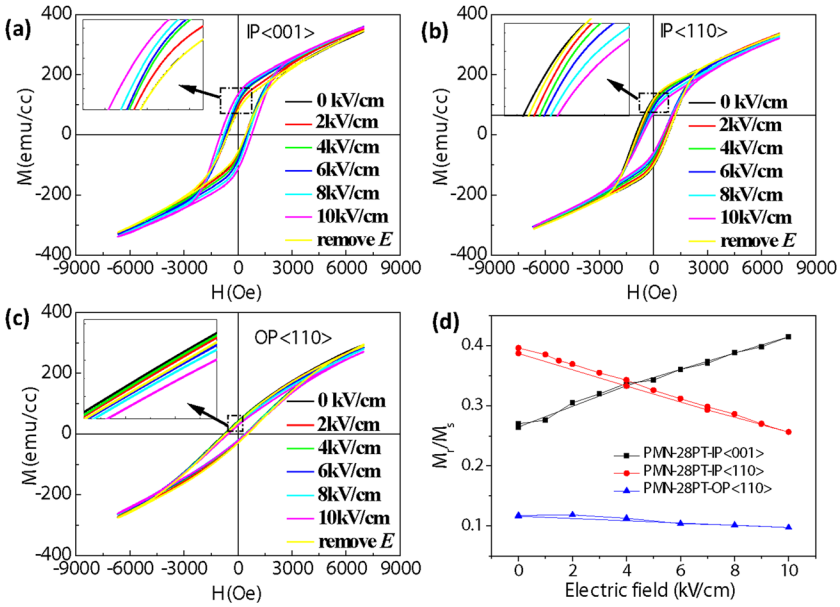

FIG. 2. M-H loops of MCFO/PMN-28PT along IP⟨001⟩ (a), IP⟨110⟩ (b), and OP⟨110⟩ (c) directions under different electric-field. (d) M_r/M_s ratio as a function of applied electric-field.

the IP⟨001⟩ direction became the magnetic easy axis due to the compressive strain for $E > 4\,kV/cm$. The OP ⟨110⟩ direction was consistently the hard axis due to the magnetic shape anisotropy. Note the linearity of the relationship between R_M and E along all the three orientations: $R_{M\text{-}ip\langle 110\rangle} = 3.9 - 0.014 \times E$, $R_{M\text{-}ip\langle 100\rangle} = 2.6 + 0.014 \times E$, and $R_{M\text{-}op\langle 110\rangle} = 1.15 - 0.001 \times E$. The magnetic strain anisotropy energy can thus be estimated to be linear with E since the R-phase is more stable in PMN-28PT.[30–34] However, the specific relationship between R_M and U_{strain} is difficult to deduce, and first principle calculations or micro-magnetic simulations are needed to develop a more detailed understanding. Interestingly, a similar linear relationship has previously been reported in Ni/PMN-PT heterostructures;[11] therefore, it is reasonable to presume that the R_M of ferromagnetic films will change in proportion to the strain applied by the piezoelectric substrate. The complete recovery of the magnetic anisotropy indicates that the polarization rotates back to the original ⟨111⟩ direction (R-phase) on removal of E.

Figure 3 shows similar magnetic property measurements for a MCFO thin film on PMN-29.5PT. Again, along IP⟨001⟩, the magnetic domains became "harder" due to an E induced compressive strain, whereas those along IP⟨110⟩ and OP⟨110⟩ became "softer" due to tensile strains. Fig. 3(d) shows the relationship between $R_M = M_r/M_s$ and E. For PMN-29.5PT, E can induce a R→O phase transition by rotating the polarization from ⟨111⟩ to OP⟨110⟩. Therefore, the remanent magnetization will experience an electric-field-sensitive initial stage for $0 < E < 5\,kV/cm$, due to the large electromechanical coupling coefficient in the polarization rotation process. The value of M_r/M_s will then become relatively stable for $E > 5.5\,kV/cm$ due to a complete R→O phase transformation. Moreover, a jump of the R_M value in the field range of $5 < E < 5.5\,kV/cm$ for all three directions was trigged by approaching the threshold of the R→O phase transformation.[26]

Figure 4 shows M-H loops for a MCFO film on PMN-30PT under various fields. The value of M_r along IP⟨001⟩

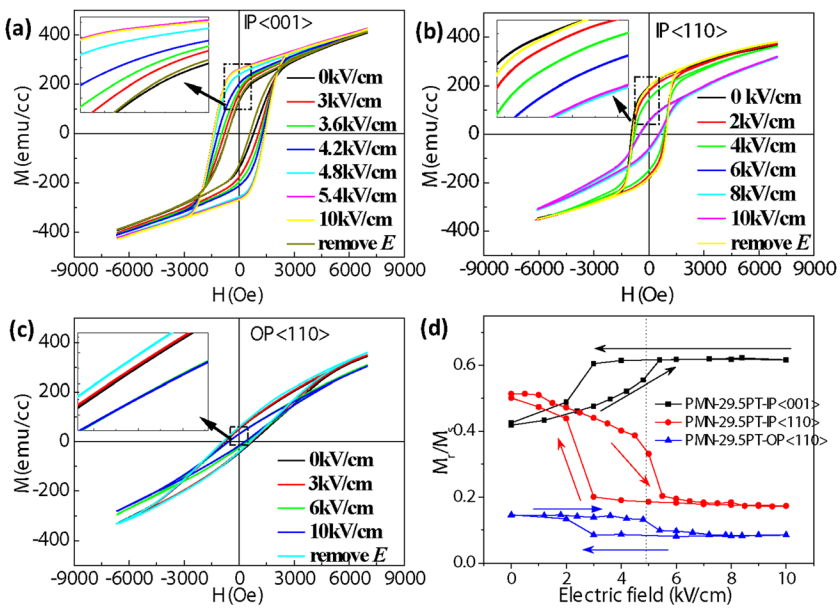

FIG. 3. M-H loops of MCFO/PMN-29.5PT along IP⟨001⟩ (a), IP⟨110⟩ (b), and OP⟨110⟩ (c) directions under different electric-field. (d) M_r/M_s ratio as a function of applied electric-field.

This article is copyrighted as indicated in the article. Reuse of AIP content is subject to the terms at: http://scitation.aip.org/termsconditions. Downloaded to IP: 128.173.125.76 On: Mon, 13 Jan 2014 20:11:51

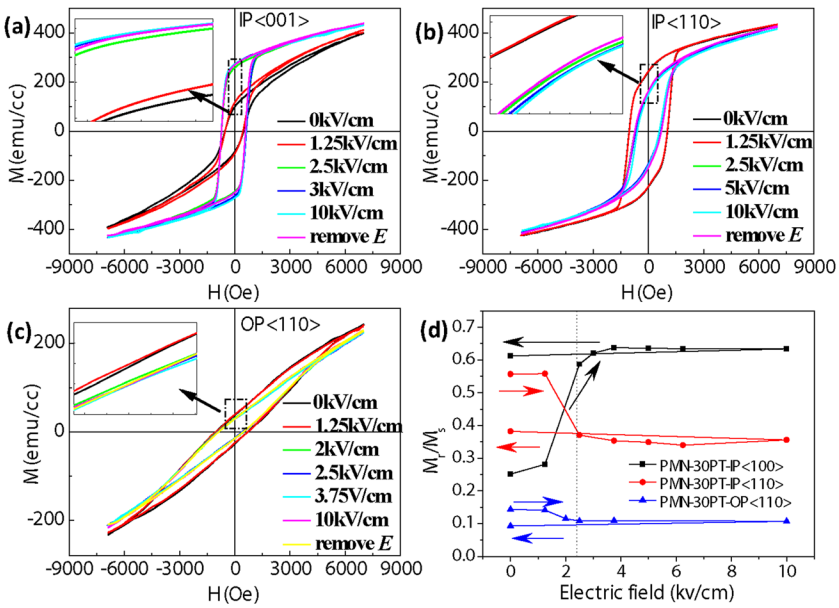

FIG. 4. M-H loops of MCFO/PMN-30PT along IP⟨001⟩ (a), IP⟨110⟩ (b), and OP⟨110⟩ (c) directions under different electric-field. (d) M_r/M_s ratio as a function of applied electric-field.

increased slowly at low fields, and then a dramatic increase was found near 2 kV/cm due to the compressive strain induced by the R→O transformation (Fig. 4(a)). At this point, the PMN-30PT is in a stable mono-domain O state, resulting in constant M_r and M_s values after removal of E. Dramatic changes in the M_r values were also found along IP⟨110⟩ and OP⟨110⟩ directions near 2 kV/cm. It is important to emphasize that the field induced strains in PMN-30PT are stable upon removal of E in the absence of another driving force. Overall, a stable field induced mono-domain O state in the PMN-30PT substrates resulted in a non-volatile converse ME effect in the MCFO films. Both reversible and irreversible converse ME effects have been detected due to the volatile and nonvolatile strains induced by electric-fields applied across PMN-PT crystals with different compositions. Next, we may ask how the magnetic anisotropy is affected by the variable strain. The magnetic anisotropy energy (E_{ani}) in a ferromagnetic thin film can be expressed as

$$U_{ani} = U_{mc} + U_{ex} + U_{shape} + U_{strain}, \quad (1)$$

where U_{mc} is the magneto-crystalline anisotropy energy, U_{ex} is the magneto-exchange anisotropy energy, U_{shape} is the magneto-static anisotropy energy, and U_{strain} is the magneto-elastic anisotropy energy.[8] U_{mc} and U_{ex} are related to the intrinsic crystal structure and specific distribution of the magnetic domains in the thin films which are difficult to manipulate, and which are beyond the scope of this paper. On the contrary, U_{strain} can be easily controlled for ferromagnetic thin films on piezoelectric substrates by electric-field.

Figure 5(a) shows the anisotropy of M_r/M_s (i.e., R_M) distribution of a MCFO thin film on PMN-28PT for different electric-field conditions. First, the MCFO film had larger remnant magnetizations along the directions diagonal to the square crystal due to a large shape anisotropy that cannot be controlled by E. Second, increased and decreased values of M_r can be found along IP⟨001⟩ and IP⟨110⟩ directions, respectively, after application of E = 10 kV/cm to the PMN-PT substrates. Third, the values of M_r were similar for MCFO/PMN-28PT heterostructure before and after application of 10 kV/cm, indicating a complete recovery of the original magnetic anisotropy condition after removal of E. These results demonstrate a reversible rotation of the magnetic easy axis from IP⟨110⟩ to IP⟨001⟩ by E. (Here, we only compared the IP⟨110⟩ and IP⟨001⟩ directions but not the diagonal ones where the M_r could not be effectively turned by E.) Fig. 5(b) shows the anisotropy of R_M for a MCFO film on PMN-29.5PT under different field conditions. Again, a reversible rotation of the magnetic easy axis from IP⟨110⟩ to IP⟨001⟩ by E was observed. The value of R_M along the IP⟨001⟩ at 10 kV/cm was 1.5 times larger than that at 0 kV/cm; whereas along the IP⟨110⟩, at 10 kV/cm, it is only 1/3 of the value that at 0 kV/cm. Fig. 5(c) shows the anisotropy of R_M for a MCFO film on PMN-30PT. Again, a

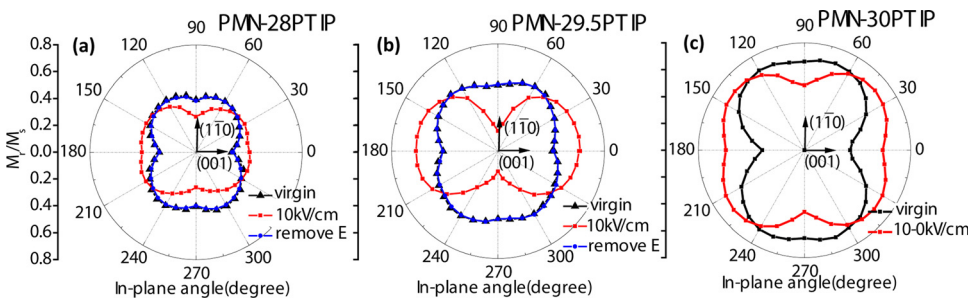

FIG. 5. M_r/M_s ratio distribution in the in-plane directions with different electric-field conditions for MCFO films on PMN-28PT, PMN-29.5PT, and PMN-30PT.

This article is copyrighted as indicated in the article. Reuse of AIP content is subject to the terms at: http://scitation.aip.org/termsconditions. Downloaded to IP: 128.173.125.76 On: Mon, 13 Jan 2014 20:11:51

rotation of the magnetic easy axis from IP⟨110⟩ to IP⟨001⟩ by E can be seen after application of 10 kV/cm to the PMN-30PT substrate. The value of R_M increased from 0.25 to 0.63 along IP⟨001⟩; whereas along IP⟨110⟩, it decreased from 0.56 to 0.36 as E increased from 0 to 10 kV/cm. Moreover, the field induced changes in M_r were preserved upon removal of E, demonstrating an irreversible magnetic easy axis rotation.

In summary, large reversible and irreversible field induced strains in PMN-PT single crystal substrates have been used to tune the magnetic anisotropy of epitaxial magnetic ferrite films. Thin films of MCFO on PMN-28PT and PMN-29.5PT exhibited a volatile strain-mediated magnetic anisotropy variation with an easy axis that changed from being along ⟨110⟩ (in-plane) to ⟨001⟩ (in-plane) under electric-field, which then recovered its original condition upon removal of E. In contrast, MCFO films on PMN-30PT exhibited a nonvolatile strain-mediated magnetic anisotropy variation with a permanent easy axis change from ⟨110⟩ (in-plane) to ⟨100⟩ (in-plane). These results clearly demonstrate a strong coupling between ferroelectric and ferromagnetic orders, and the volatile and nonvolatile magnetic anisotropy tunabilities may provide additional approaches to magnetic memory and spintronic applications.

This work was supported by U.S. Department of Energy (DE-FG02-06ER46290).

[1]W. Eerenstein, M. Wiora, J. L. Prieto, J. F. Scott, and N. D. Mathur, Nature Mater. **6**, 348 (2007).
[2]R. Ramesh and N. A. Spaldin, Nature Mater. **6**, 21 (2007).
[3]J. Das, Y.-Y. Song, N. Mo, P. Krivosik, and C. E. Patton, Adv. Mater. **21**, 2045 (2009).
[4]H. Zheng, J. Wang, S. E. Lofland, Z. Ma, L. Mohaddes-Ardabili, T. Zhao, L. Salamanca-Riba, S. R. Shinde, S. B. Ogale, F. Bai, D. Viehland, Y. Jia, D. G. Schlom, M. Wuttig, A. Roytburd, and R. Ramesh, Science **303**, 661 (2004).
[5]S. Dong, J. Zhai, J. Li, and D. Viehland, Appl. Phys. Lett. **89**, 252904 (2006).
[6]J. Zhai, J. Li, D. Viehland, and M. I. Bichurin, J. Appl. Phys. **101**, 014102 (2007).
[7]J. Zhai, Z. Xing, S. Dong, J. Li, and D. Viehland, J. Am. Ceram. Soc. **91**, 351 (2008).
[8]N. A. Pertsev, Phys. Rev. B **78**, 212102 (2008).
[9]J.-M. Hu and C. W. Nan, Phys. Rev. B **80**, 224416 (2009).
[10]J. M. Hu, Z. Li, L. Q. Chen, and C. W. Nan, Adv. Mater. **24**, 2869 (2012).
[11]T. Wu, A. Bur, K. Wong, J. L. Hockel, C.-J. Hsu, H. K. D. Kim, K. L. Wang, and G. P. Carman, J. Appl. Phys. **109**, 07D732 (2011).
[12]Z. Wang, Y. Yang, R. Viswan, J. Li, and D. Viehland, Appl. Phys. Lett. **99**, 043110 (2011).
[13]Z. Wang, R. Viswan, B. Hu, J.-F. Li, V. G. Harris, and D. Viehland, J. Appl. Phys. **111**, 034108 (2012).
[14]M. Liu, O. Obi, J. Lou, Y. Chen, Z. Cai, S. Stoute, M. Espanol, M. Lew, X. Situ, K. S. Ziemer, V. G. Harris, and N. X. Sun, Adv. Funct. Mater. **19**, 1826 (2009).
[15]J. Lou, M. Liu, D. Reed, Y. Ren, and N. X. Sun, Adv. Mater. **21**, 4711 (2009).
[16]J.-M. Hu, Z. Li, L.-Q. Chen, and C.-W. Nan, Nat. Commun. **2**, 553 (2011).
[17]X. B. Ren, Nature Mater. **3**, 91 (2004).
[18]S. E. Park and T. R. Shrout, J. Appl. Phys. **82**, 1804 (1997).
[19]C. Thiele, K. Dorr, S. Fahler, L. Schultz, D. C. Meyer, A. A. Levin, and P. Paufler, Appl. Phys. Lett. **87**, 262502 (2005).
[20]J. J. Yang, Y. G. Zhao, H. F. Tian, L. B. Luo, H. Y. Zhang, Y. J. He, and H. S. Luo, Appl. Phys. Lett. **94**, 212504 (2009).
[21]J. A. Paulsen, A. P. Ring, C. C. H. Lo, J. E. Snyder, and D. C. Jiles, J. Appl. Phys. **97**, 044502 (2005).
[22]C. H. Kim, Y. Myung, Y. J. Cho, H. S. Kim, S.-H. Park, J. Park, J.-Y. Kim, and B. Kim, J. Phys. Chem. C **113**, 7085 (2009).
[23]H. X. Fu and R. E. Cohen, Nature **403**, 281 (2000).
[24]F. Li, S. J. Zhang, Z. Xu, X. Y. Wei, and T. R. Shrout, Adv. Funct. Mater. **21**, 2118 (2011).
[25]B. Noheda, D. E. Cox, G. Shirane, J. Gao, and Z. G. Ye, Phys. Rev. B **66**, 054104 (2002).
[26]M. Shanthi and L. C. Lim, Appl. Phys. Lett. **95**, 102901 (2009).
[27]L. H. Luo, H. X. Wang, Y. X. Tang, X. Y. Zhao, Z. Y. Feng, D. Lin, and H. S. Luo, J. Appl. Phys. **99**, 024104 (2006).
[28]Y. P. Guo, H. S. Luo, T. H. He, H. Q. Xu, and Z. W. Yin, Jpn. J. Appl. Phys., Part 1 **41**, 1451 (2002).
[29]See supplementary material at http://dx.doi.org/10.1063/1.4823539 for the dielectric constant measurements of poled PMN-PT substrates in both heating and cooling process.
[30]Y. Lu, D. Y. Jeong, Z. Y. Cheng, Q. M. Zhang, H. S. Luo, Z. W. Yin, and D. Viehland, Appl. Phys. Lett. **78**, 3109 (2001).
[31]S. Zhang, N. P. Sherlock, R. J. Meyer, Jr., and T. R. Shrout, Appl. Phys. Lett. **94**, 162906 (2009).
[32]J. Peng, H. S. Luo, D. Lin, H. Q. Xu, T. H. He, and W. Q. Jin, Appl. Phys. Lett. **85**, 6221 (2004).
[33]D. Viehland, J. F. Li, and A. Amin, J. Appl. Phys. **92**, 3985 (2002).
[34]Z. Wang, Y. Li, R. Viswan, B. Hu, V. G. Harris, J. Li, and D. Viehland, Acs Nano **7**, 3447 (2013).

This article is copyrighted as indicated in the article. Reuse of AIP content is subject to the terms at: http://scitation.aip.org/termsconditions. Downloaded to IP: 128.173.125.76 On: Mon, 13 Jan 2014 20:11:51